1-s2.0-S1876610215016367-main

DATASET · AUGUST 2015

6 AUTHORS, INCLUDING:

Nicola Pastore
Politecnico di Bari
27 PUBLICATIONS **61** CITATIONS
SEE PROFILE

Claudia Cherubini
University of Queensland
33 PUBLICATIONS **75** CITATIONS
SEE PROFILE

Jose Manuel Redondo
Polytechnic University of Catalonia
210 PUBLICATIONS **893** CITATIONS
SEE PROFILE

Ana M. Tarquis
Universidad Politécnica de Madrid
232 PUBLICATIONS **852** CITATIONS
SEE PROFILE

Available online at www.sciencedirect.com

ScienceDirect

Energy Procedia 76 (2015) 273 – 281

Energy Procedia

European Geosciences Union General Assembly 2015, EGU

Division Energy, Resources & Environment, ERE

Experimental study of heat transport in fractured network

N. Pastore[a]*, C. Cherubini[b], C. I. Giasi[a], N. M. Allegretti[a,b], J. M. Redondo[d,e], A. M. Tarquis[c,d]

[a]*DICATECh - Politecnico di Bari, via E. Orabona, 70125 Bari, ITALY*
[b]*Hydrise, Institut Polytechnique LaSalle Beauvais, 19 rue Pierre Waguet, 60026 Beauvais Cedex, France*
[c]*CEIGRAM, Universitad Politécnica de Madrid - iudad Universitaria Madrid, 28040 Spain*
[d]*PELNoT, ERCOFTAC, Instituto Pluridisciplinar, Paseo Juan XXIII, 1, 28040, Madrid, Spain*
[e]*Dept. Fisica Aplicada, Univ. Politecnica de Cataluña, 08034, Barcelona, Spain*

Abstract

Fractured rocks play an important role in transport of natural resources through subsurface systems. In recent years, interest has grown in investigating heat transport by means of tracer tests, driven by the important current development of geothermal applications. Many field and laboratory tracer tests in fractured media show that fracture - matrix exchange is more significant for heat than mass tracers, thus thermal breakthrough curves are strongly controlled by matrix thermal diffusivity. In this study, the behaviour of heat transport in a fractured network, at bench laboratory scale, has been investigated.

Peer-review under responsibility of the GFZ German Research Centre for Geosciences

Keywords: heat transport; fractured rock, physical model

1. Introduction

The aim of this paper is investigate the behaviour of heat transport in fractured media. The laws that govern the heat transport in fractured media are still little known and there are not many experiences in literature about these

* Corresponding author. Tel.: +39-080-596-3371 ; fax: +39-080-596-3414 .
E-mail address: nicola.pastore@poliba.it

Peer-review under responsibility of the GFZ German Research Centre for Geosciences
doi:10.1016/j.egypro.2015.07.860

phenomena. Existing theory of fluid flow and heat transport through porous media is of limited usefulness when applied to fractured rocks.

Nomenclature

a	linear coefficient of Forchheimer's law (TL^{-3})
b	inertial coefficient of Forchheimer's law (T^2L^{-6})
BTC	thermal breakthrough curve
C	conductance term (L^2T^{-1})
C_w	specific heat capacity of the water ($L^2T^2K^{-1}$)
C_m	specific heat capacity of the matrix ($L^2T^2K^{-1}$)
d	distance along z axis from fracture – matrix interface (L)
δ	thickness of boundary layer (L)
ENM	explicit network model
D_f	thermal dispersion coefficient (L^2T^{-1})
h	hydraulic head (L)
j	single vertical fracture index
k_e	effective thermal conductivity of the matrix ($MLT^{-3}K^{-1}$)
L	length of single fracture or characteristic length of fracture network (L)
L^{-1}	inverse Laplace transform operator
n_f	number of single fracture
N_p	number of paths
P_Q	probability of water distribution of shorter parallel branch
PDF	probability of density function of residence time
Q	flow rate (L^3T^{-3})
Q_0	injection flow rate (L^3T^{-3})
ρ_w	density of water (ML^{-3})
ρ_m	density of the matrix (ML^{-3})
Re	Reynolds number (-)
s	Laplace parameter (-)
SF	vertical single fracture
t_u	convective time scale (T)
t_d	dispersion time scale (T)
t_e	transfer time scale (T)
T_f	fracture temperature (K)
T_m	matrix temperature (K)
T_0	initial temperature (K)
T_{inj}	injection temperature (K)
u_f	thermal convective velocity (LT^{-1})
x	coordinate parallel to the axis of vertical single fracture
w_f	fracture aperture (L)
z	coordinate perpendicular to the fracture axis (L)
$*$	convolution operator

Fractured rocks play an important role in transport of natural resources or contaminants transport through subsurface systems. In recent years, interest has grown in investigating heat transport by means of tracer tests, driven by the important current development of geothermal applications.

In particular way low enthalpy geothermal resource is an optimal renewable resource because is always available and it is possible used for the heating and cooling of private buildings, industries, public buildings, representing the largest share of world energy consumption.

The study of heat transport in fractured aquifers, which represent the 75% of the earth's surface, is crucial in order to understand the possible advantages and disadvantages resulting from the use of aquifers as low enthalpy geothermal resources.

A laboratory study, at bench scale, has been conducted on an artificially created fractured limestone block of parallelepiped shape. Some holes have been drilled on the block, inside which the temperature probe has been inserted. The observed thermal *BTCs* have been modeled with the explicit network model (*ENM*) based on an adaptation of Tang's solution, developed for solute transport in a semi – infinite single fracture embedded in a porous matrix.

Characteristic transport time scale has been compared in order to evaluate the dominant mechanism on heat propagation in fractured media.

2. Theoretical background

2.1. Flow and heat transport in single fractures

A fracture can be depicted as two rough surfaces in contact. Cross sectional solid areas representing asperities in contact are similar to the grains of porous media. It is therefore possible to apply the general equations describing flow and heat transport in porous as well as in fractured media.

In most studies examining hydrodynamic processes in fractured media, it is assumed that flow is described by Darcy's law, which expresses a linear relationship between pressure gradient and flow rate [1]. Darcy's law has been demonstrated to be valid at low flow regimes ($Re < 1$). For $Re > 1$, a nonlinear flow behaviour is likely to occur [2].

In the literature different laws are reported that account for the nonlinear relationship between velocity and pressure gradient. In case of higher Reynolds numbers ($Re \gg 1$) the pressure losses pass to a strong inertial regime, described by the Forchheimer's law [3]. The relationship between flow rate and hydraulic head gradient can be written as:

$$-\frac{dh}{dx} = a \cdot Q + b \cdot Q^2 \tag{1}$$

A *SF* is subject to fluid flow with an averaged velocity, heat will migrate by convection and diffusion phenomena along the fracture. Furthermore they will also undergo dispersion caused by small scale variations in fracture aperture.

One dimensional advective - dispersive transport along the fracture axis, as well as one – dimensional diffusion in the rock matrix, in direction perpendicular to the axis of the fracture is considered. Assuming that density and heat capacity are constant in time, conservation equation can be written for heat transport in a semi - infinite fracture as:

$$\frac{\partial T_f}{\partial t} + u_f \frac{\partial T_f}{\partial x} = \frac{\partial}{\partial x}\left(D_f \frac{\partial T_f}{\partial x} \right) - \frac{k_e}{\rho_w C_w \delta} \frac{\partial T_m}{\partial z}\bigg|_{z=w_f/2} \tag{2}$$

Whereas the conservation equation for heat transport in the matrix is:

$$\rho_m C_m \frac{\partial T_m}{\partial t} = k_e \frac{\partial^2 T_m}{\partial z^2} \tag{3}$$

[4] and [5] propose a thermal dispersion coefficient similar to the solute transport, where the thermal dispersion term is related to the heterogeneity and it is a linear function of velocity.

[6] presents a solution for solute transport in semi – infinite single fracture surrounded by porous matrix for a constant concentration at the fracture inlet ($x = 0$) and for initial concentration equal to zero everywhere. They give the expression for the solute concentration in the fracture and in the matrix as function of time. On the basis of this analytical solution, the *PDF* in the single fracture in the Laplace space can be written as:

$$\bar{\Gamma}(s) = \exp(vL)\exp\left[-vL\left\{1+\beta^2\left(\frac{s^{1/2}}{A}+s\right)\right\}^{1/2}\right] \tag{4}$$

Whereas the *PDF* in the matrix in the Laplace space assumes the following expression:

$$\bar{\Gamma}'(s) = \bar{\Gamma}(s)\cdot\exp\left(-Bs^{1/2}d\right) \tag{5}$$

The coefficients v, A, β^2 and B assume the following expressions:

$$v = \frac{u_f}{2D_f};\ \beta^2 = \frac{4D_f}{u_f};\ B = \frac{1}{\sqrt{D_e}} \tag{6}$$

$$A = \frac{\delta}{\sqrt{\theta D_e}};\quad \theta = \frac{\rho_m C_m}{\rho_f C_f},\quad D_e = \frac{k_e}{\rho_w C_w} \tag{7}$$

2.2. Explicit network model

A vertical *SF* can be viewed as one dimensional pipe element in which head loss is described by Forchheimer's law. The conductance to flow of the generic *SF j* can be written as:

$$C_j = \left[L_j\left(a_j + b_j Q_j\right)\right]^{-1} \tag{8}$$

The flow field in the fracture network can be determined in analytical way through the application of the first and the second Kirchhoff's laws. The flow rate crossing generic *SF j* can be obtained as the product between the total discharge flow ΣQ_i, evaluated for the fracture intersection located at the inlet bond of the *SF j*, and the probability of flow distribution of *SF j* $P_{Q,j}$. The latter is equal to the ratio between the conductance to flow of *SF j* and the sum of conductance to flow of each discharge *SF* connected at the inlet bond of *SF j*, as well as $P_{Q,j}$ should be proportional to the relative discharge flow rates:

$$P_{Q,j} = \frac{C_j}{\sum_{i=1}^{n} C_i} = \frac{Q_j}{\sum_{i=1}^{n} Q_i} \tag{9}$$

The *PDF* at a generic node can be obtained as the summation of *PDFs* of each elementary path that reach the node. The latter is equal to the convolution product of the *PDFs* of each single fracture along the elementary path.

The *BTC* that describe the temperature in the fracture at the generic node of the fracture network is:

$$T_f(t) = T_0 + T_{inj}(t) * L^{-1}\left[\sum_{i=1}^{N_p}\prod_{j=1}^{n_{f,i}} P_{Q,j}\bar{\Gamma}_j(s)\right] \tag{10}$$

Whereas the temperature in the matrix evaluated at distance d along z axis from fracture – matrix interface at the generic node is:

$$T_m(t) = T_0 + T_{inj}(t) * L^{-1}\left\{\left[\sum_{i=1}^{N_p}\prod_{j=1}^{n_{f,i}} P_{Q,j}\bar{\Gamma}_j(s)\right]\exp\left(-Bs^{1/2}d\right)\right\} \tag{11}$$

3. Material and methods

3.1. Experimental setup

The experiments have been performed on the laboratory physical model used to study flow and solute transport at bench scale [7, 8, 9, 10, 11]. In Fig. 1 is reported the schematic diagram of the experimental setup.

In order to analyze the heat transport dynamics in the fractured sample, some modifications have been made. The same sealed fractured limestone block with parallelepiped shape (0.6×0.4×0.08 m^3), described in previous work, has been used. A hole of 2 mm diameter has been opened up to the depth of 1 cm along the center of some discontinuities by means of a percussion drill. Inside of each opened hole a thermocouple has been placed and welded to the block by means of rapid – hardening epoxy resin. Furthermore at the inlet and the outlet of the selected path other two thermocouples have been placed. All thermocouples have been connected to a TC-08 Thermocouple Data Logger (Pico Technology) and a sampling rate of 1 second has been used.

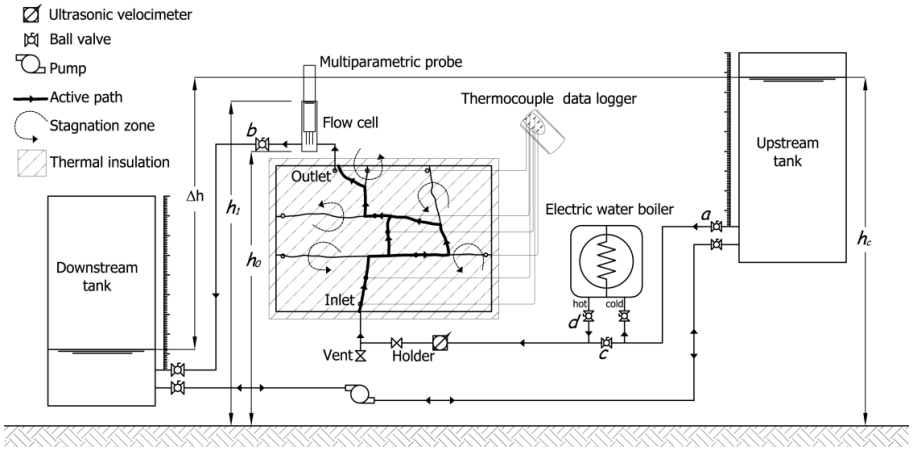

Fig. 1. Schematic diagram of the experimental setup.

The limestone block has been thermally insulated using extruded polystyrene panel with thermal conductivity equal to 0.034 $Wm^{-1}K^{-1}$ and thickness 0.05 m. Finally the sample has been connected to a hydraulic circuit. Water inside the sample flows according to the hydraulic head difference between the upstream tank connected to the inlet port and the downstream tank connected to the outlet port. The instantaneous flow rate that flows across the block is measured by an ultrasonic velocimeter (DOP3000 by Signal Processing). Water that enters into the sample is heated by an electric water boiler with a volume of 10^{-2} m^3. In correspondence of outlet port there is a flow cell in which a multiparametric probe is positioned for instantaneous measurement of pressure (dbar), temperature (°C) and electric conductivity (μS cm^{-1}).

3.2. Temperature tracer tests

The study of heat transport dynamics has been carried out through a selected path. Initially a hydraulic head difference between the upstream tank and the downstream tank is imposed. At time $t = 0$ the valve "*a"* is closed and hydrostatic head inside the block is equal to the downstream tank. At time $t = 10$ s the valve "*a"* is opened while at time $t = 60$ s the valve "*d*" is opened and in the same time the valve "*c"* is closed. In this manner, a step temperature function is imposed in correspondence of the inlet port T_{inj} (t) and it is measured by the thermocouple inside the inlet port. At time $t = 1000$ s the valve "*d"* and the valve "*c"* are reclosed and reopened respectively. For different flow rates *BTCs* curves have been recorded at the inlet and output ports and inside the sample in correspondence of some discontinuities.

4. Results and discussion

The Forchheimer parameters representative of the whole fracture network were derived in [11]. The estimated Forchheimer parameters are respectively $a = 7.345\times10^{4}$ sm^{-3} and $b = 11.65\times10^{9}$ $s^{2}m^{-6}$. The critical flow rate corresponding to the ratio between the linear and nonlinear term equal to the unit in which the inertial force dominate viscous one is equal to $Q_{crit} = 6.30\times10^{-6}$ $m^{3}s^{-1}$. The probability of water distribution of each *SF* is equal to one except for the parallel branches. The probability of water distribution of the shorter parallel branch P_Q decreases as the injection flow rate increases because, due to the nonlinear nature of flow, the conductance term of the shorter parallel branch decreases faster than the conductance term of the longer parallel branch.

The observed *BTCs* have been fitted by *ENM* based on Tang's solution. The parameters u_f, D_f, D_e and δ are supposed equal for the all branches except for the parallel branches in which u_f and D_f become $u_f P_Q$ and $D_f P_Q$ for the shorter branch and $u_f (1 - P_Q)$ and $D_f (1 - P_Q)$ for the longer branch. The thermal *BTC* in correspondence of the outlet port is fitted using equation (10), whereas the thermal *BTCs* at the position inside the block is fitted by equation (11) using a distance along z - axis from fracture - matrix interface d equal to the dimension of thermocouple (2 mm).

Fig. 2 shows the fitting results of thermal *BTCs* at different positions along the fracture network for the injection flow rate equal to $Q_0 = 4.03\times10^{-6}$ m^3/s. The fitting was satisfactory, except for the positions 2 and 3 in which the *ENM* model underestimates the observed thermal *BTCs* curves. The *ENM* model results able to represent the behaviour of observed heat transport except where the configuration of the fracture network gives rise to a fracture block characterized by a limited capability to store heat. In this configuration, the Tang's solution fails to model the observed thermal transport in correspondence of parallel branch, because the porous matrix surrounding the single fracture cannot be considered infinite in size. The thermal *BTCs* in parallel branches are influenced each other. As a consequence the observed *BTCs* show a lower heat dissipation then *ENM* model. Initially the hypothesis of infinite porous matrix is still valid, the *ENM* model reaches observed *BTCs*. Subsequently the observed *BTCs* begin to influenced each other giving rise to lower heat dissipation, resulting that the *ENM* model underestimate the observed *BTCs*.

According to [12] the following three characteristics transport time scale can be defined as:

$$t_u = \frac{L}{u_f};\ t_d = \frac{L^2}{D_f};\ t_e = \frac{\delta^2}{\theta D_e} \tag{12}$$

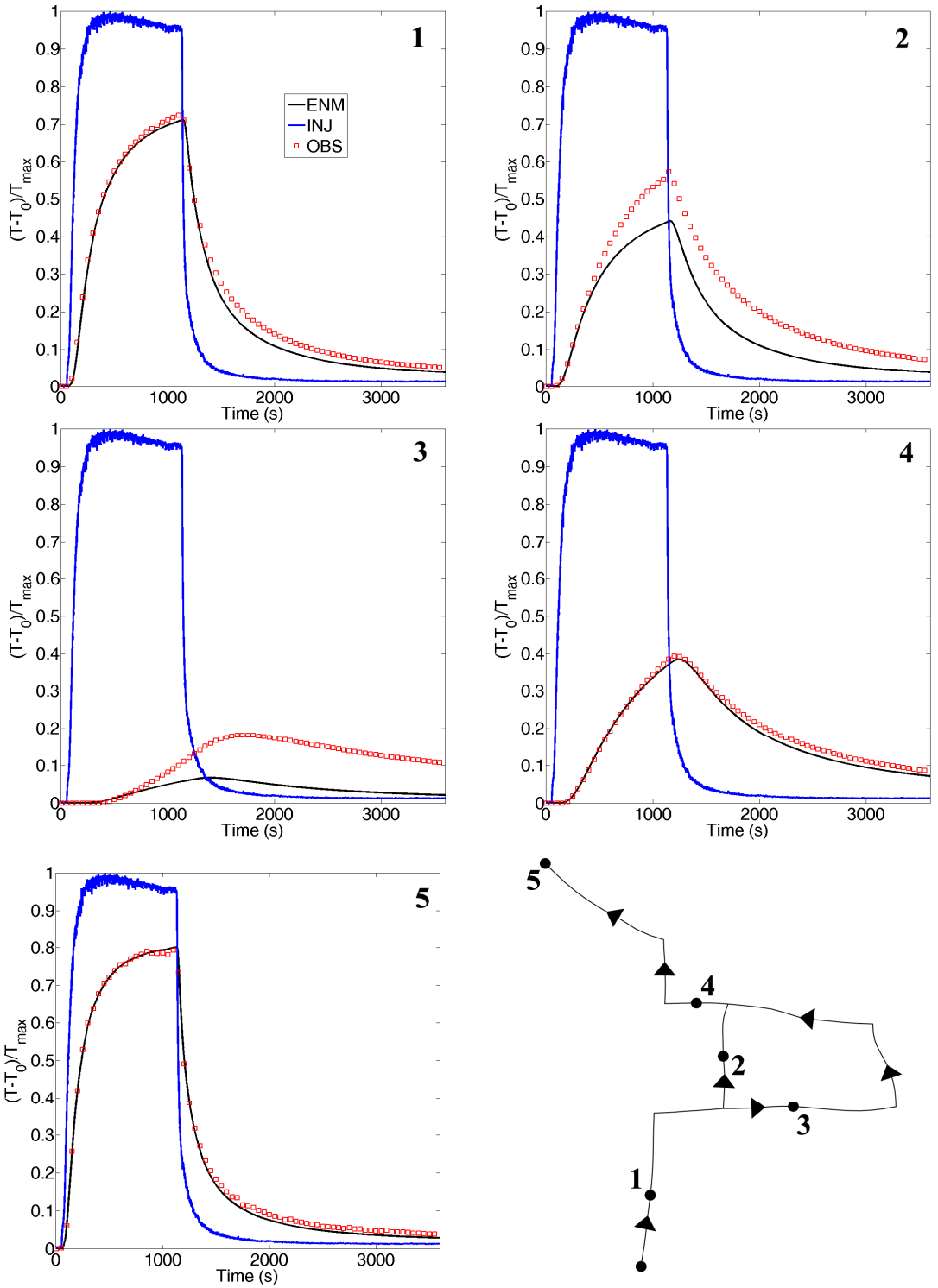

Fig. 2. Fitting of BTCs at different positions in the fracture network using ENM with Tang solution for heat transport with injection flow rate equal to $Q_0 = 4.03 \times 10^{-6}$ m^3/s.

Table 1 shows the estimated transport time scale at different injection flow rates.

According to previous works the characteristic length of fractured media is equal to L = 0.601 m. Convective transport time scale is the same order of magnitude of the exchange time scale, the impact of the fracture matrix exchange is very strong giving rise to a strong retardation effect on the convective velocity.

Table 1. Estimated values of parameters for ENM with Tang solution at different injection flow rates.

Q_0 (m^3s^{-1})×10^{-6}	t_u (s)	t_d (s)	t_e (s)
1.84	240	182	297
2.32	251	190	240
2.68	234	198	273
2.85	245	178	256
3.00	231	157	317
4.00	226	54	879
4.22	143	40	349
7.06	72	35	318
7.96	61	19	164
8.97	44	15	115
12.36	53	16	352
12.59	40	14	164

The thermal dispersion plays an important role on heat transport dominating on convective transport, although the injection flow rate is relatively high. Infact, dispersion time scale is always less than convective time scale. Furthermore, dispersion time scale and exchange time scale are comparable. However, the latter is always less than the former.

The comparison with previous studies on solute transport carried out in fractured media shows that thermal *BTCs* are characterized by a more enhanced early arrival and long tailing than solute *BTCs*. The residence time t_m for heat transport is an order of magnitude higher than for solute transport experiments. Fig. 2 shows the comparison of the observed residence times versus the injection flow rates both solute and heat transport. These results highlight that the heat transport is more retarted than mass transport.

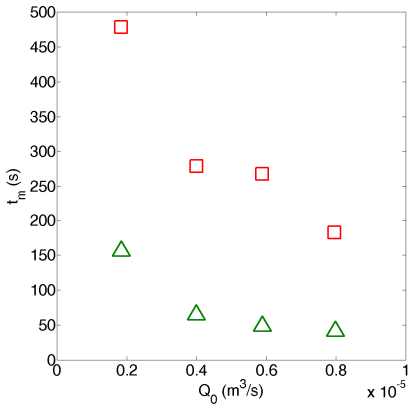

Fig. 2. Comparison between the residence time t_m of heat transport (red square) and solute transport (green triangle) at different injection flow rate Q_0.

5. Conclusion

Several features on the behaviour of heat transport have been observed by the conducted experiments and their interpretation.

Heat transport dynamics have been fitted by the explicit network model with Tang's solution. *ENM* model exhibits a satisfactory fitting except in correspondence of the parallel branch in which the porous matrix surrounding the single fracture cannot be considered infinite in size. The Parallel branches are influenced by each other as a consequence the observed *BTCs* show lower heat dissipation than *ENM* model.

Heat transfer time scale is comparable with convective time scale because the dual porosity behaviour is very strong, giving rise to a delay on heat propagation in fracture network.

Thermal *BTCs* are characterized by a more enhanced early arrival and long tailing than solute *BTCs* observed in previous experiments. The residence time of heat transport is an order of magnitude higher than the residence time of solute transport.

Thermal dispersion time scale is always less than both thermal convective time scale and thermal exchange time scale. These results confirm that thermal dispersion plays an important role on heat transport and its effect cannot be neglected.

The results encourage further experimental work to increase the knowledge of the key parameters that govern the heat propagation in fractured media, and therefore developing the best strategies for installation of devices for heat recovery and heat dissipation in fractured media.

References

[1] Cherubini C, Pastore N. Modeling contaminant propagation in a fractured and karstic aquifer. Fresenius Environmental Bulletin 2000; 19 (9) p. 1788-1794.

[2] Cherubini C, Giasi CI, Pastore N. Fluid flow modeling of a coastal fractured karstic aquifer by means of a lumped parameter approach. Environmental Earth Sciences 2013; 70 (5) p. 2055-2060.

[3] Forchheimer P. Wasserbewegung durch Boden. Z. Ver. Dtsch. Ing. 1901; 45 p. 1781-1788.

[4] Sauty JP, Gringarten AC, Fabris H, Thiery D, Menjoz A, and Landel PA. Sensible energy storage in aquifers 2. Field experiments and comparison with theoretical results. Water Resources Research 1982; 18 (2) p. 253–265.

[5] deMarsily G. Quantitative Hydrogeology: Groundwater Hydrology for Engineers. Academic Press; 1986.

[6] Tang DH, Frind EO, Sudicky EA. Contaminant transport in fractured porous media: analytical solutions for a single fractures. Water Resources Research 1981; 17 (3) p. 555-564.

[7] Cherubini C, Giasi CI, Pastore N. Bench scale laboratory tests to analyze non-linear flow in fractured media. Hydrology and Earth System Sciences 2012; 16 p. 2511-2622.

[8] Cherubini C, Giasi CI, Pastore N. Evidence of non-Darcy flow and non-Fickian transport in fractured media at laboratory scale. Hydrology and Earth System Sciences 2013; 17 p. 2599-2611.

[9] Cherubini C, Giasi CI, Pastore N. Laboratory tests to analyze solute transport behaviour in fractured media. Rendiconti Online Società Geologica Italiana 2013; 24 p. 55-57.

[10] Cherubini C, Giasi CI, Pastore N. Un modello fisico di laboratorio per analizzare dinamiche di flusso e trasporto in un campione di roccia fratturata a scala di banco [A laboratory physical model to analyse flow and transport processes in fractured rock sample at bench scale level]. Italian Journal Engineering Geology and Environment 2013; (1) p. 19-32.

[11] Cherubini C, Giasi CI, Pastore N. On the reliability of analytical models to predict solute transport in a fracture network. Hydrology and Earth System Sciences 2014; 18 p. 2359-2374.

[12] Kocabas I. Geothermal reservoir characterization via thermal injection backflow and interwork tracer testing. Geothermics 2005; 34 p. 27-46.